Proceedings of the 9th U.S. National and 10th Canadian Conference on Earthquake Engineering
Compte Rendu de la 9ième Conférence Nationale Américaine et
10ième Conférence Canadienne de Génie Parasismique
July 25-29, 2010, Toronto, Ontario, Canada • Paper No 525

EXPERIMENTAL INVESTIGATION OF THE CYCLIC BEHAVIOUR OF UNREINFORCED MASONRY SPANDRELS

K. Beyer[1], A. Abo El Ezz[2] and A. Dazio[3]

ABSTRACT

In unreinforced masonry (URM) walls the vertical piers are connected by horizontal spandrel elements. Numerical simulations have shown that spandrels influence significantly the global wall behaviour under seismic loading. Despite their importance, experimental data on the cyclic behaviour of these spandrels is very scarce. The lack of experimental data prevented in the past the validation of numerical and mechanical models regarding the cyclic behaviour of masonry spandrels. For this reason a research program was initiated in which the cyclic behaviour of masonry spandrels was investigated experimentally and numerically. Within this program different configurations of masonry spandrels were tested under quasi-static monotonic and cyclic loading. The spandrel configurations that were investigated included pure masonry spandrels and masonry spandrels which also comprise a reinforced concrete (RC) beam or slab. The latter represents spandrels in newer masonry buildings with RC slabs or RC ring beams while the former can be found in older masonry buildings. This paper presents preliminary results of the experimental program as well as some selected results of the accompanying numerical study.

Introduction

Over the past decades the seismic action defined in the Swiss design codes has steadily increased. For this reason – despite the moderate seismicity of Switzerland – it is today virtually impossible to design unreinforced masonry (URM) buildings for seismic loading or to verify the seismic safety existing URM buildings. This applies to some extent even to zones of low seismicity with design peak ground accelerations of 10% g and less. It is generally accepted that most of the design approaches for URM structures in today's design codes are rather conservative. For example, most design approaches neglect the framing action due to the horizontal spandrel elements and consider only the vertical pier elements when calculating the strength and stiffness of the URM wall. Numerical simulations have, however, shown that the spandrel elements influence significantly the force-deformation characteristics of a URM wall. A major reason why spandrel elements are not considered in the design of URM structures is the

---

[1] Post-doctoral researcher, beyer@ibk.baug.ethz.ch, Institute of Structural Engineering, ETH Zurich, Switzerland.

[2] Graduate Research Assistant, aboelezz@ibk.baug.ethz.ch, Institute of Structural Eng., ETH Zurich, Switzerland.

[3] Assistant Professor, Institute of Structural Engineering, dazio@ibk.baug.ethz.ch, ETH Zurich, Switzerland.

lack of experimental evidence for the behaviour of masonry spandrels under seismic loading. At present research efforts in Italy at the University of Trieste (Gattesco et al. 2008) and at the EUCentre in Pavia are underway that investigate experimentally the behaviour of URM and stone masonry spandrels, respectively. A research project was also initiated at the ETH Zurich with the aim to improve the characterisation of the force-deformation relationships of spandrels in URM buildings. The results of the experimental program will be used to develop mechanical models for the load-bearing and deformation behaviour of spandrels in URM buildings as well as to refine the global analysis of URM walls. The final goal is to develop practice-oriented guidelines for the modelling of spandrels when performing pushover analysis of URM walls with and without reinforced concrete slabs. The results of the pushover analysis can be used to remove some conservatism of the current force-based design approaches or they can form the basis for a displacement-based design of URM walls; the latter has the potential to lead to more rational and economic structures than force-based design.

Within the research project several large-scale test units of different types of spandrels were tested under quasi-static loading. The experimental program was divided into two parts. The test units of the first part represented spandrels in more modern URM buildings while in the second part spandrels of older URM buildings were tested. The major differences between the two parts of the test program concern (i) the presence or absence of a reinforced concrete (RC) beam in the first and second part, respectively, and (ii) the brick type. The test units representing spandrels in modern URM buildings were constructed with larger bricks with holes while for the test units representing spandrels in old buildings with wooden floors smaller bricks without holes were used. The latter test units included either a wooden lintel and a masonry spandrel or a masonry spandrel with a shallow arch to bridge the opening. In this paper only the first part of the experimental study is presented together with some selected results of pushover analyses on URM buildings as well as analysis results for isolated spandrel beams.

Different Types of Spandrels in Modern URM Buildings

Modern URM buildings are often constructed with RC slabs or RC ring beams. The spandrel elements of the latter differ from the former mainly regarding the stiffness and strength of the RC element. In buildings with RC slabs three different types of spandrels in the facade can be distinguished: (i) Spandrel consisting of masonry, RC slab and RC or reinforced masonry lintel (Figure 1a). This type of a spandrel is typically found in older buildings with RC slabs. The more recent the construction the larger the window openings tend to be. (ii) Often the lintel disappears all together and the window frame and the roller shutter casing reach up to the RC slab (Figure 1b). (iii) In very recent buildings even the masonry spandrel above the slab often disappears and the window unit reaches over the entire storey height (Figure 1c). In this case, the coupling of the masonry piers results only from the RC slab. A similar coupling mechanism can be found in inner walls where the coupling action due to the RC slab is sometimes reinforced by a door lintel. In view of the large variety of spandrel elements in modern URM buildings it is impossible to conduct large-scale tests on all types of spandrels. Since tests serve chiefly for the validation of numerical models, it was decided to concentrate on spandrel elements with masonry and RC slabs. It is assumed that models that are able to capture the behaviour of masonry spandrels as shown in Figure 1b can also capture the behaviour of the other two types of spandrels.
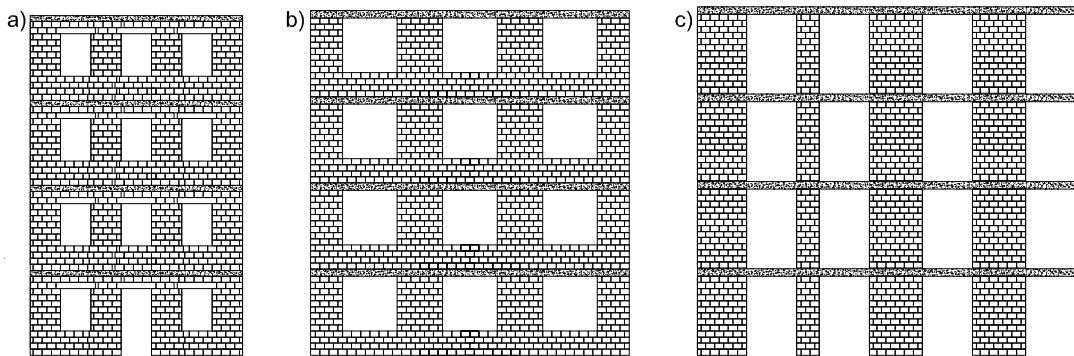
Figure 1.   Facades of masonry buildings with RC slabs and different spandrel types: Spandrels consisting of masonry spandrel, RC slab and lintel (a), of masonry spandrel and RC slab (b) and of a RC slab only (c).

Numerical Simulation of URM Walls and Isolated Spandrels

The URM walls and test units were analysed using the finite element program "Atena" (Cervenka 2007). This program was chosen since it includes very advanced material models for concrete and reinforcing steel. In addition, masonry can be modelled by means of a simple heterogenous micro model where each brick is modelled as an elastic unit and the mortar joints are represented by contact elements with a Mohr-Coulomb friction law (Löring 2005). Although this modeling approach results in quite detailed models, it has a number of drawbacks: (i) Failure of the bricks cannot be captured since the bricks are modelled as elastic. In typical Swiss masonry, however, the mortar joints fail typically far earlier than the bricks. Brick failure can be important when determining the displacement capacity of the spandrels. For this reason, the employed model can at best yield rough estimates of the deformation capacity of the spandrel elements. (ii) Since the joints are modelled as infinitely thin, effects resulting from the different Poisson's ratios of bricks and mortar cannot be captured. The experimental results have, however, confirmed that this simplification is in most cases acceptable.

Pushover-Curve of a 3-Storey URM Wall

To support the planning of the experimental campaign several 3-storey URM walls were analysed (Beyer and Dazio 2008). In the following the results of a pushover analysis on a URM wall with three 3.0 m long piers, spandrels with a length of 1.5 m and a free storey height of 2.40 m are discussed. In this particular case, the RC slab is replaced by a ringbeam with a thickness of 0.24 m and a width of 0.20 m, which corresponds to the width of the masonry wall. The longitudinal reinforcement of each RC beam consists of 4 D12 mm bars, the shear reinforcement of D6 mm hoops with a spacing of 150 mm. In the two lower storeys the spandrel consists, apart from the RC beam, of four rows of bricks. The pushover analysis of the URM wall was performed with a triangular load distribution over the height of the wall. The loads were applied at the centerlines of the RC beams and the distribution of the loads was kept constant throughout the analysis. In addition to the horizontal loads, vertical loads were applied which simulated the self-weight of piers and slabs as well as an additional distributed load on the
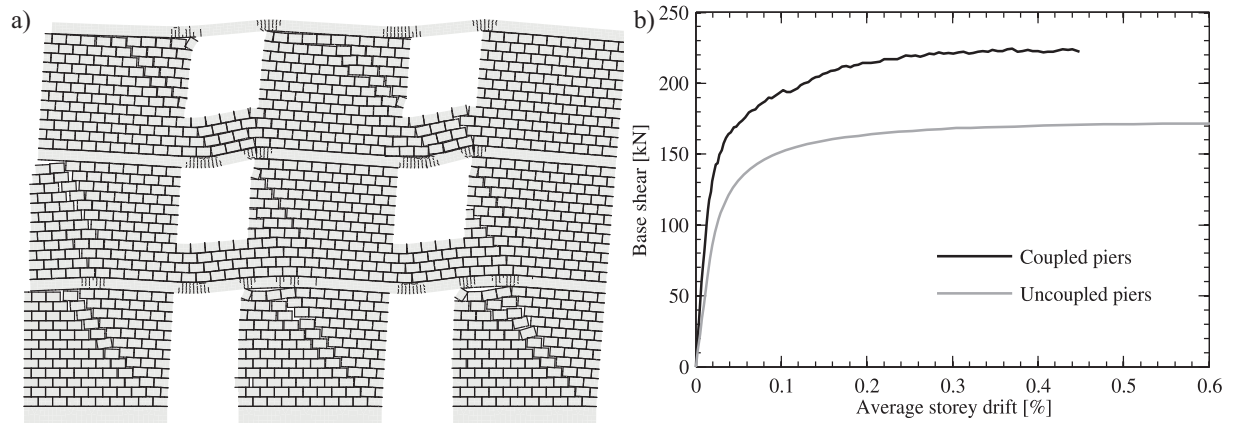
Figure 2.   Deformed shape of the URM wall at an average storey drift of δ=0.4% (a, displacements are magnified by a factor of 20) and pushover curve of the URM wall in comparison to the pushover curve of uncoupled piers (b).

slab. Figure 2a shows the deformed shape of the URM wall at an average storey drift of δ=0.4%. The average storey drift was calculated as the horizontal displacement of the top floor slab divided by the height of the wall. The cracks in the RC beams indicate the locations where plastic hinges are forming in the beams: The plastic hinge with negative moment (for the direction of loading shown in Figure 2a it is the right hinge of each spandrel) is located above the edge of the piers. This is also the expected location of plastic hinges is URM walls where no masonry spandrels are present and where the piers are only coupled by RC beams (Figure 1c). The positive plastic hinge, on the contrary, is not located at the edge of the pier but is shifted inside the free span of the spandrel. This is because the compression strut, which is propped on the hinge, can shift for the here shown direction of loading to the right due to the presence of the masonry spandrel above the RC beam. As a consequence the effective span of the spandrel is shortened and the resistance of the spandrel is increased when compared to a spandrel consisting of a RC beam alone. Figure 2b compares the pushover curve of the URM wall in Figure 2a to the pushover curve of three uncoupled piers, i.e. the curve when the coupling action of the spandrel elements is neglected. The figure shows that the spandrel elements have a significant influence on the initial stiffness as well as on the resistance of the URM wall.

Pushover-Curve of an Isolated Spandrel

The test units consist of a single spandrel as well as adjacent parts of the piers. The latter are required for the application of the forces to the spandrel and for guaranteeing as realistic boundary conditions of the spandrel as possible. It was checked by means of Atena simulations that the chosen test setup yields a similar demand on the spandrel as the URM wall in Figure 2. Figure 3 shows the deformed shape and the pushover curve of the test unit for a storey drift of δ=0.4%. The spandrel itself has the same dimensions as the spandrel in the URM wall in Figure 2a. The URM piers on the left and right of the spandrel are, however, only 2.1 m long; for this reason the demands on the spandrel in Figure 2 and Figure 3 are not exactly the same for the same storey drift. The comparison of the deformed shapes in Figure 2 and 3 show, however, that the boundary conditions of the spandrel in the test unit are on the whole very similar to those in a URM wall.

a)

b)
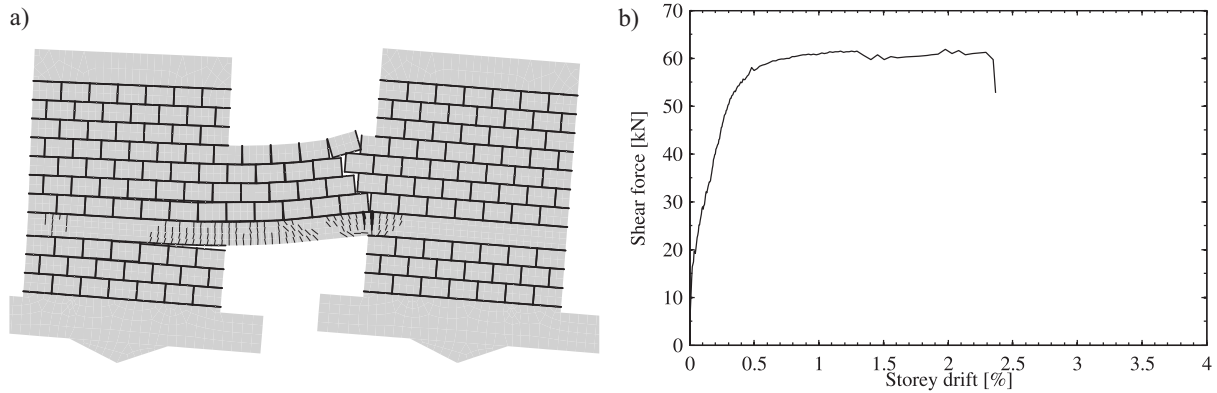
Figure 3.   Deformed shape of a spandrel test unit at a drift of δ=0.4% (a, displacements are magnified by a factor of 20) and pushover curve of the test unit (b).

Test Units, Test Setup and Loading History

Test Units

The first part of the experimental program, i.e. the part addressing spandrels which included RC beam, comprised the testing of five units. The dimensions of the test units were identical and are shown in Figure 4a. Table 1 lists for all test units with RC beam the type of loading, the longitudinal reinforcement of the RC beam and the type of the bricks that was used for the construction of the test unit. The first two test units were tested under a monotonic loading scheme. When assessing the seismic behaviour, cyclic loading as it was used for Test Units TU3-5 is more representative. However, design approaches are often based on pushover analyses. While it is known that for ductile RC elements the pushover curve obtained from monotonic loading corresponds well with the envelope obtained from cyclic loading, this assumption does not always holds for URM elements and should therefore be justified. For this reason, two identical test units (TU2 and TU3) were subjected to monotonic and cyclic loading, respectively, and the results obtained compared.

Table 1.   Loading scheme, reinforcing and brick details of the five test units.

	Loading	Reinforcement of RC Beam	Masonry Brick
TU1	Monotonic	4 D12 mm (4.52 cm^2)	Type 1
TU2	Monotonic	4 D12 mm (4.52 cm^2)	Type 2
TU3	Cyclic	4 D12 mm (4.52 cm^2)	Type 2
TU4	Cyclic	4 D16 mm (8.04 cm^2)	Type 2
TU5	Cyclic	4 D10 mm (3.14 cm^2)	Type 2

The difference between TU1 and TU2 consists in the type of bricks used. While the bricks of TU1 had non-continuous longitudinal webs, the bricks of TU2 had continuous longitudinal webs (Figure 4b and c). The Swiss Masonry Code (SIA 266, 2003) does not

regulate the form of the webs and therefore both types bricks are used in Switzerland. On the contrary, the Italian Seismic Design Code (OPCM 3431, 2005) specifies, however, that only bricks with continuous longitudinal webs may be used. TU4 and TU5 differ from the other test units regarding the longitudinal reinforcement of the RC beams, which was 4 D16 mm and 4 D10 mm bars, respectively, compared to the 4 D12 mm bars of TU1-3. The Italian Seismic Design Code (OPCM 3431, 2005) requires for RC ring beams a minimum longitudinal reinforcement area of 8 cm^2, which corresponds to 4 D16 mm bars, and a minimum beam width equal to the width of the masonry wall. For the shear reinforcement a minimum of D6 mm hoops every 250 mm must be provided. TU4 therefore satisfies all the minimum requirements of a ring beam according to OPCM 3431 (2005); only the shear reinforcement is with D6 mm hoops every 150 mm slightly larger than required. According to the European Seismic Design Code EC8 (CEN 2004) a ring beam has to be fitted with a minimum longitudinal reinforcement area of 2 cm^2; this is considerably smaller than the reinforcement area of TU1-4. For this reason a fifth beam was tested with less longitudinal reinforcement (TU5).
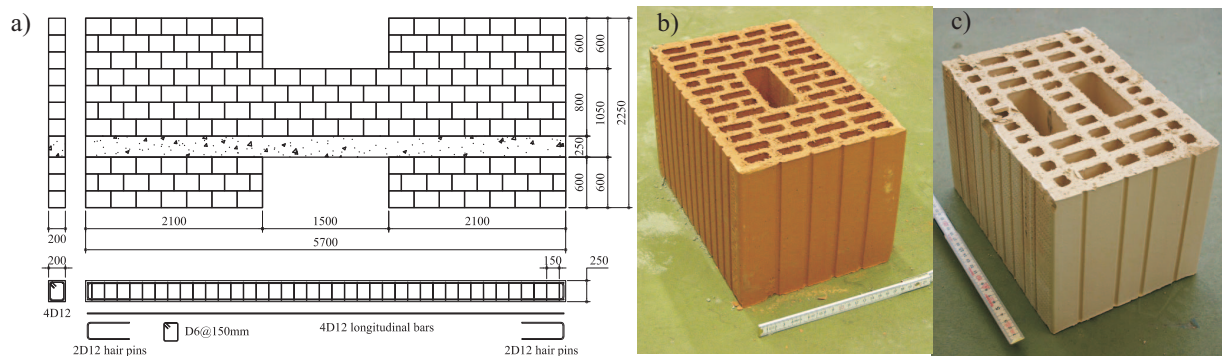
Figure 4.   Dimensions of the test units and reinforcement of the RC beams. The longitudinal reinforcement varied between the test units according to Table 1 (a), brick type 1 and 2 with non-continuous and continuous longitudinal webs, respectively (b, c).

Test Setup and Instrumentation

The test setup is shown in Figure 5. The test unit stands on two stiff steel beams that are supported on hinges at the centre of the piers and connected to servo-hydraulic actuators at the beam ends. Both actuators are displacement-controlled. The support of the South beam allows next to a rotation also a sliding movement in the direction of the beam. Hence, no axial forces can develop within the spandrel. During testing the actuators are moved with the same velocity in opposite directions. As a result the two horizontal beams rotate and the piers right and left to the spandrel are subjected to the same drift, which causes the demand on the spandrel. From the actuator forces and the reaction forces at the hinges the shear force within the spandrel can be calculated. Before the testing is initiated an axial load of 160 kN is applied to each pier by means of four prestressed rods. Different global and local deformation quantities as well as actuator and reaction forces were measured during testing by means of 58 hard-wired channels. In addition to these hard-wired channels, the East faces of the test unit and of the test setup were equipped with 196 LEDs. The LEDs were used to measure the coordinates by means of an optical measurement system (NDI OptotrakCertus HD).
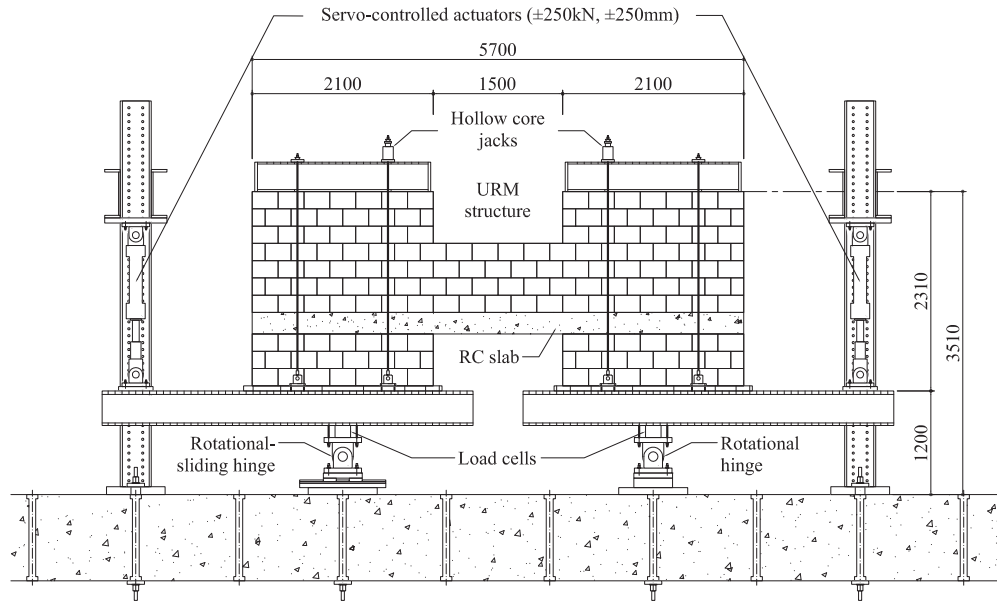
Figure 5.   East face of the test setup (Note: To improve the readability of the drawing the lateral support system to restrain the test unit from excessive out-of-plane movement is not shown).

Loading History

Both the monotonic and the cylic loading scheme followed different steps of storey drifts. Force-based load steps, which are often used at the beginning of quasi-static cyclic tests of RC elements, were not considered. Force-based load steps are typically used to determine a yield displacement which forms the basis of the stepwise increase of the displacement amplitude in the then following displacement-based cycles. Determining a yield displacement is already difficult and ambiguous for RC elements; it is even less clear for URM elements. For this reason the loading history was solely controlled by different storey drift levels and the applied storey drift levels were the same for all test units. The storey drift corresponds to the rotation of the two horizontal beams, which were identical throughout the test. The rotation of the beams were determined by means of LVDTs mounted between the beams and the strong floor. When the monotonic loading scheme was applied, the loading was stopped at the following storey drift levels: 0.025%, 0.05%, 0.1%, 0.2%, 0.3%, 0.4%, 0.6%, 0.8%, 1.0%, 1.5%, 2.0%, 2.5%, 3.0%, 4.0%. The same levels determined the amplitudes of the cyclic loading scheme. At each level the test unit was subjected to two loading cycles.

Experimental Results

The detailed analysis of the test results is currently underway. For this reason only the first results of two out of the five experiments are presented and discussed here. The two selected test units are TU2 and TU3, which differ only regarding the applied loading scheme (see Table 1): TU2 was subjected to monotonic loading and TU3 to cyclic loading. The longitudinal reinforcement of the RC beams consists in both cases of 4 D12 mm bars; therefore the experimental results can be directly compared to the numerical results presented at the beginning of this paper.

Failure Mechanism

Although TU2 and TU3 differed only regarding the loading scheme to which the test unit were subjected the failure mechanism of the two test units was different. TU2 failed at approximately 3.5% storey drift due to fracture of the longitudinal reinforcement in the RC beam (Figure 6a). A bar of the top layer fractured within the negative plastic hinge shortly before a bar of the bottom layer fractured within the positive plastic hinge. These two bar ruptures marked the end of the test. At this point the spandrel shear force was reduced to approximately one fourth of the maximum spandrel shear force. The masonry of the spandrel was separated by two wide stair stepped cracks and only the masonry wedge located left of the left crack contributed to the resistance of the spandrel by allowing the compression diagonal to reach within the spandrel. Only the bricks which were part of this strut were damaged and partly failed; all other bricks remained virtually undamaged and all deformations were concentrated within the cracks. Test Unit TU3 failed within the first cycle at a storey drift of 3% due to shear failure of the RC beam. At approximately 55 cm from the left edge of the spandrel a shear hoop fractured within a diagonal crack which had widened considerably during the last cycles. Since the test setup did not provide any constraint against axial elongation of the test unit (see Section "Test setup"), the length of the test unit increased during the cyclic loading within the plastic range. For this reason the shear transfer due to aggregate interlock across the shear cracks within the RC beam reduced and led eventually to the shear failure. The crack pattern and damage to the masonry was similar to that of TU2. The cyclic instead of the monotonic loading contributed to a more pronounced weakening of the bond between bricks and the crack widths were more evenly distributed over the spandrel.
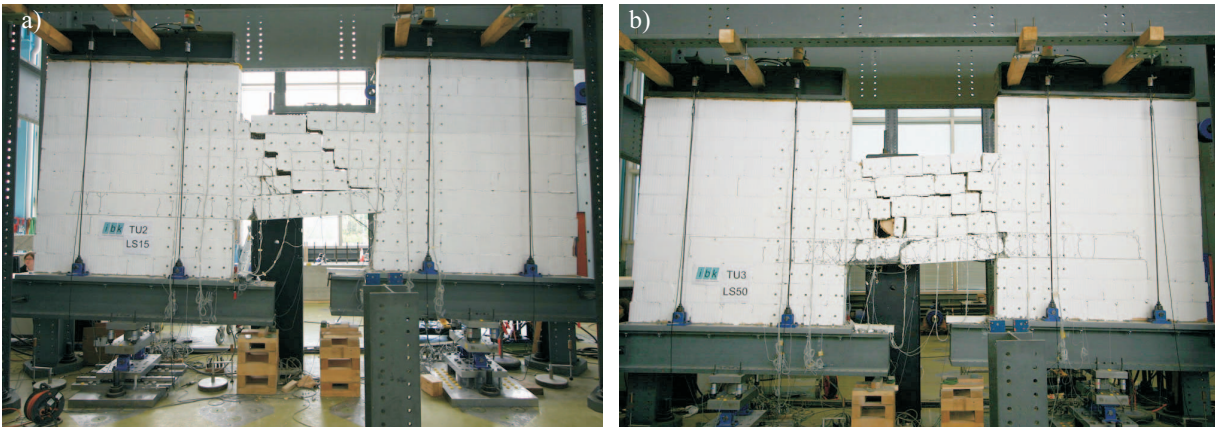
Figure 6.   Test units at the end of the experiments: TU2 after monotonic loading (a) and TU3 after cyclic loading (b).

Force-Deformation Relationship

Figure 7 shows the force-deformation relationships of TU2 and TU3 in comparison to the results of two different theoretical models. The first model is the Atena-model presented in the Section "Pushover-curve of an isolated spandrel". The second model is based on a simple hand calculation assuming that only the RC beam and not the masonry spandrel contributes to the

spandrel resistance. The resistance of the RC beam is calculated assuming that a plastic hinge forms at each end of the spandrel and the maximum shear force of the spandrel without masonry is calculated as $V=2M_n/l_{sp}$ where M_n is the nominal flexural strength of the RC beam, which was computed using the program "Response2000" (Bentz 2000), and l_{sp} the free span of the spandrel, i.e. 1.5 m. The comparison of the force-deformation curves of TU2 and TU3 shows that the envelope of TU3 corresponds well with the force-deformation curve of TU2. Similar values are even obtained for the displacement capacity although the failure mechanisms are different. The very large displacement capacity should, however, be taken with some reservation. First, during a real earthquake the spandrel is also subjected to out-of-plane loading and loose bricks would therefore fall off. Second, according to common assumptions (e.g. EC8, Part 3 (CEN 2005)), the piers would have failed long before the spandrel and therefore the boundary conditions of the spandrel would no longer correspond to the rather undamaged piers as seen in Figure 6a and b.
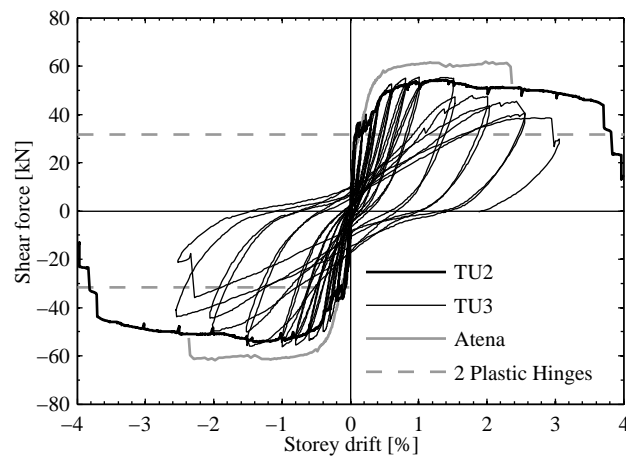
Figure 7.   Force – deformation relationship of TU2 and TU3 compared to the results of the Atena model and a model based on the strength of the RC beam alone.

The Atena analysis overestimates the force-capacity of the spandrels by about 15% which is considered acceptable for such elements. The Atena model is therefore considered a suitable model for the prediction of the behaviour of spandrel elements with RC beams. The resistance that was computed on the basis of the plastic hinge model underestimates the capacity of the spandrel considerably. This shows that the masonry should not be neglected when striving for realistic force-displacement relationships of such spandrel elements. This is particularly important if the RC beam is intended to be capacity-designed since the masonry leads to larger shear forces in the RC beam and hence – as it was the case for TU3 – possibly to a shear failure rather than the preferred flexural failure.

Conclusions

The five tests on spandrel test units with RC beams showed (i) that the masonry of the spandrel affects the load bearing mechanism of the spandrel and increases the strength and stiffness of the spandrel considerably, and (ii) that the failure mechanism as well as the strength capacity of the spandrel can be estimated in an adequate manner by means of the developed Atena models. The experiments also showed that the deformation capacity of the spandrel elements is quite large and exceeds for typical spandrel configurations the design storey drifts of

piers of either 0.4% (shear failure, CEN 2005) or 0.8% (flexural failure, CEN 2005) considerably. The experiments could, however, not consider any effects due to out-of-plane loading. Next steps of this project concern the detailed analysis of the experimental data and the development of simple mechanical models for estimating the force-displacement characteristics of such spandrel elements. The second part of the experimental program, which is currently under way, addresses the behaviour of spandrels in old URM buildings with wooden slabs.

Acknowledgments

References

Bentz, E.C., 2000. Response 2000 – Reinforced Concrete Sectional Analysis using the Modified Compression Field Theory, *User Manual*, University of Toronto, Canada.

Beyer, K., and Dazio, A., 2008. Analysis of coupled masonry walls, *Report*, Institute of Structural Engineering, ETH Zürich, Switzerland.

CEN, 2004. *Eurocode 8: Design of structures for earthquake resistance – Part 1: General rules, seismic actions and rules for buildings*. EN 1998-1. European Committee for Standardization, Brussels, Belgium.

CEN, 2005. *Eurocode 8: Design of structures for earthquake resistance – Part 3: General rules, seismic actions and rules for buildings*. EN 1998-3. European Committee for Standardization, Brussels, Belgium.

Cervenka, V., 2007. Atena – Computer Program for Nonlinear Finite Element Analysis of Reinforced Concrete Structrues, *Theory and User Manual*, Prague, Czech Republic.

Gattesco, N., Clemente, I., Macorini, L. and Noè, S., 2008. Experimental investigation of the behaviour of spandrels in ancient masonry buildings, *Proc. of the 14th World Conference on Earthquake Engineering*, Beijing, China.

Löring, S., 2005. Zum Tragverhalten von Mauerwerksbauten unter Erdbebeneinwirkung (On the load bearing behaviour of masonry structures under seismic loading), *PhD dissertation*, Universität Dortmund, Germany.

OPCM n. 3431, 2005. Ulteriori modifiche ed integrazioni all'OPCM n. 3274 del 20 marzo 2003, recante „Primi elementi in materia di criteri generali per la classificazione sismica del territorio nazionale e di normative tecniche per le costruzioni in zona sismica". Suppl. Ordinario n. 85 alla G.U. n. 107 del 10 maggio 2005. Ordinanza del Presidente del Consiglio dei Ministri del 3 maggio 2005. Rome, Italy.

SIA 266 (2003), *Mauerwerk (Masonry)*, Design Code, Schweiz. Ingenieur- und Architektenverein, Zurich, Switzerland.